BMC Infectious Diseases

RESEARCH

Open Access

Antibiotic resistance and viral co-infection in children diagnosed with pneumonia caused by *Mycoplasma pneumoniae* admitted to Russian hospitals during October 2023—February 2024

Elena Korneenko[1*†], Irina Rog[1†], Ivan Chudinov[1,2†], Aleksandra Lukina-Gronskaya[1], Anfisa Kozyreva[1], Ilmira Belyaletdinova[1,3], Julia Kuzmina[1], Oleg Fedorov[1], Daria Evsyutina[1], Alexey Shunaev[1], Daria Matyushkina[1], Vadim Govorun[1,2] and Anna Speranskaya[1,4]

Abstract

Background *Mycoplasma pneumoniae* (MP) is a common bacterial respiratory infection that can cause pneumonia, particularly in children. Previously published data have highlighted the high incidence of viral co-infections and the problem of increasing macrolide resistance in MP worldwide.

Aims (1) to estimate the impact of viral infections circulating in a local population on the spectrum of co-infection in hospitalized children with *Mycoplasma pneumoniae* pneumonia (MPP), (2) to determine if there are differences in resistance mutation rate for samples from hospitals of Russia located in the European and Far East, (3) to describe genomic characteristics of MP from Russian patients during the MPP outbreaks in the fall-winter of 2023–2024.

Methods The carriage of viral pathogens was analyzed by real-time PCR in children with MPP from the European Part and Far East of Russian Federation and compared with the infections from two control groups. The V region of the *23S* gene and the quinolone resistance-determining regions (QRDRs) of the *parC* and *gyrA* genes were sequenced to detect resistance-associated mutations in MP. Whole-genome sequencing method was used to determine the genetic relationship of a Russian MP isolate with known MP isolates.

Results The 62% of patients with MPP had a viral co-infection, with HPIV and SARS-CoV-2 predominating at 47% and 12.4%, respectively. The 15% of patients were infected with two or more viruses. In the control groups, 21% of healthy children and 43% of healthy adults were infected with Coronaviruses and Human Parainfluenza Viruses (HPIV-3 and -4), respectively. The 2063 A/G mutation of the *23S* gene was found in 40.8% of patients from European Russia and in 35.7% of patients from the Far East. The result of core genes demonstrates that the sequence obtained from Russia clusters with sequences from clade 1.

†Elena Korneenko, Irina Rog and Ivan Chudinov contributed equally to this work and share first authorship.

*Correspondence:
Elena Korneenko
lenakorneenko0@gmail.com
Full list of author information is available at the end of the article

Conclusions Both HPIV and SARS-CoV-2 circulated in the population among healthy children and adults in December 2023 and they also were predominated in children with MPP. The rate of macrolide resistance was ~40%, which is higher than in European countries and significantly lower than in patients from Asian countries. Phylogenetic analysis showed the MP genome form Russia related to P1 type 1 (clade 1).

Keywords *Mycoplasma pneumoniae*, Macrolide resistance, Viral co-infection, Coronaviruses, SARS-CoV-2, Human Parainfluenza Viruses, HPIV-3, HPIV-4

Introduction

Mycoplasma pneumoniae (MP) is one of the smallest self-replicating and cell-wall-less bacteria, that can cause respiratory infections in children and adults, that is transmitted by airborne droplets through contact in homes and public places [1]. Symptoms of *M. pneumoniae* infection are highly variable, with manifestations ranging from non-specific symptoms of an upper respiratory tract infection to atypical pneumonia. Pneumonia caused by *M. pneumoniae* (MPP) is most commonly observed in children and adolescents [2]. *M. pneumoniae* infection occurs in different seasons, and the number of detected cases usually increases from summer to early spring, with a peak in winter [3, 4]. Climatic factors such as temperature and humidity may contribute to the seasonal variation in the incidence rate of *M. pneumoniae* [4–6]. Outbreaks of disease caused by *M. pneumoniae* occur globally every 3–7 years, with each outbreak lasting 1–2 years [4, 7]. The last previous outbreak of *M. pneumoniae* infection before the COVID-19 pandemic occurred in late 2019 or early 2020, with most reports coming from countries in Europe and Southeast Asia [8].

The introduction of non-pharmaceutical interventions against COVID-19 in March 2020 is widely regarded as a contributing factor to the observed decline in the global *M. pneumoniae* infection rate. Currently, the global surveillance data showed the re-emergence of local *M. pneumoniae* infection outbreaks in Europe and Asia, after the delay during the COVID-19 pandemic [9, 10]. In the third year of the COVID-19 pandemic, an increase in the number of *M. pneumoniae*-positive patients was observed in some countries, although at very low levels since last months of 2022 [9–15]. An increase of the *M. pneumoniae* infection (without details) was mentioned for the Russian Federation, in the fall of 2023, in the short report by [16] (in russian).

Several authors suggest that co-infections with various viral and bacterial pathogens can increase the severity of *Mycoplasma pneumoniae* respiratory infections [17–20]. The prevalence of viral or bacterial pathogens in patients with *Mycoplasma pneumoniae* pneumonia (MPP) has been documented in multiple studies [17–23]. Current research focuses on antibiotic-resistant strains of *M. pneumoniae*. Macrolides are the first-line treatment for *M. pneumoniae* respiratory tract infections due to their low minimum inhibitory concentrations, low toxicity, and lack of contraindications in young children [24]. However, fluoroquinolones and tetracyclines, which are contraindicated in children due to their side effects, remain the only viable alternatives for treating infections caused by macrolide-resistant strains until new effective drugs are developed [25]. Macrolides target the 23S rRNA, and resistance is primarily associated with mutations in the V domain of this gene. The most prevalent mutations that result in high-level resistance to 14- and 15-membered macrolides are located at positions 2063 (A > G, A > T) and 2064 (A > G, A > C), while mutations at positions 2067 (A > G) and 2617 are linked to low-level resistance [26–29]. Fluoroquinolones target topoisomerase IV (*parC* gene which encodes a subunit of topoisomerase IV) and DNA gyrase (*gyrA*). In the *parC* gene, missense mutations at positions 78, 79, 80, and 84 which are associated with fluoroquinolone resistance, have been reported in *M. pneumoniae*, *M. genitalium*, and *Ureaplasma urealyticum* (Mycoplasmataceae) [30–32]. Furthermore, mutations at position 83, a known "hot spot" for fluoroquinolone resistance in *Escherichia coli*, have been observed in moxifloxacin-resistant strains of *M. pneumoniae*, *Mycoplasma hominis*, and *Ureaplasma* species [32–34]. Although mutations in the quinolone resistance-determining regions (QRDRs) of the *gyrA* gene have not been described for *M. pneumoniae*, they have been identified in fluoroquinolone-resistant strains of *Mycoplasma genitalium*, the closest relative of *M. pneumoniae*, as well as in other mycoplasmas [30, 31]. Therefore, QRDRs is a promising target for the search of new mutations of resistance to fluoroquinolones.

In this study, we investigated mutations associated with antibiotic resistance and viral co-infections in children hospitalized with MPP in Russia during the autumn–winter season of 2023–2024. We also performed genotyping and, for the first time, complete genome characterization of *M. pneumoniae* isolate from the Russian patient using microbiological cultivation methods, whole genome amplification (WGA) and high-throughput sequencing (HTS).

Materials and methods

Sample collection

All samples (nasopharyngeal swabs or sputum) investigated in this study were collected between October 19, 2023 and February 21, 2024.

The experimental group, consisting of children diagnosed with *Mycoplasma pneumoniae* pneumonia (hereafter "children with MPP"), included 193 samples. Patients were enrolled in the study based on the following criteria: (1) Age less than 18 years; (2) Hospitalization with a diagnosis of J15.7 Pneumonia caused by *Mycoplasma pneumoniae*. The diagnosis was confirmed by clinical symptoms of pneumonia, such as fever, cough; physical examination findings, including rales in the lungs; imaging studies demonstrating lung inflammation; and a positive PCR test result for *M. pneumoniae*.

Nasopharyngeal swabs and sputum samples were collected from children diagnosed with MPP across 16 regions of the Russian Federation. The sample distribution was as follows: Novgorod region ($n=26$), Volgograd region ($n=8$), Voronezh region ($n=3$), Lipetsk region ($n=9$), Nizhny Novgorod region ($n=3$), Amur region ($n=27$), Republic of Chuvashia ($n=11$), Kostroma region ($n=4$), Yaroslavl region ($n=2$), Sverdlovsk region ($n=15$), Komi Republic ($n=4$), Tver region ($n=1$), Tula region ($n=10$), Mari El Republic ($n=9$), Moscow ($n=46$), and Moscow region ($n=15$). Sample collection from patients is carried out within 1–2 days from the moment of admission to the hospital.

Two control groups were included in the study. Control group 1 (Healthy Children, $n=38$): included participants based on the following criteria: age under 18 years; absence of significant clinical symptoms of respiratory disease at the time of sample collection. Control group 2 (Healthy Adults, $n=72$) included participants based on the following criteria: age over 18 years; absence of significant clinical symptoms of respiratory disease at the time of sample collection.

Nasopharyngeal swabs were obtained from participants in both control groups as part of a voluntary research study, with informed consent provided and signed by all participants.

Real-time PCR testing

In hospitals, real-time PCR testing for *Mycoplasma pneumoniae* was performed on 193 samples obtained from hospitalized children diagnosed with MPP. The quantitative method with the *Mycoplasma pneumoniae/Chlamydophila pneumoniae*-FRT kit (AmpliSens, Russia), considered values below a Ct of 33 as positive. Alternatively, the qualitative method with the *Mycoplasma pneumoniae/Chlamydophila pneumoniae*-FEP kit (AmpliSens, Russia) was used. A subset of samples from patients diagnosed with MPP was subjected to testing for *Mycoplasma pneumoniae* using the POLYMIC 1 reagent kit (Litech, Russia), with a Ct cut-off range of 5 to 40 considered positive.

For samples from control group 1 and control group 2 nucleic acids (RNA and DNA) were extracted from all samples using the MagMAX Viral/Pathogen Nucleic Acid Isolation Kit (Applied Biosystems, USA) on the KingFisher Apex automated isolation system. Real-time PCR was conducted to detect viral pathogens and *Mycoplasma pneumoniae*. Detection of *Mycoplasma pneumoniae* for both control groups was performed using the POLYMIC 1 reagent kit (Litech, Russia). Viral infections were evaluated using non-commercial PCR kits developed by the RnD Department of Litech, Russia. The targets included: adenoviruses (types A-G), rhinoviruses, coronaviruses (HKU1, OC43, 229E, NL63), respiratory syncytial viruses (RSV types A and B), bocavirus (hBoV), metapneumoviruses (MPV), parainfluenza viruses (HPIV types 1–4), and influenza viruses (types A and B), with a Ct cut-off range of 5 to 40 considered positive.

A real-time PCR kit (Syntol, Russia) was used to detect SARS-CoV-2 nucleic acids, considering values below a Ct of 50 as positive.

Statistical analyses

Statistical analyses were conducted using MS Office Excel 365 (Microsoft, USA). The two-tailed Fisher's exact test with Bonferroni correction was applied to compare the prevalence of viral infection.

Amplification of the V region of the 23S rRNA gene (associated with macrolide resistance in bacteria)

Primers targeting the V region of the 23S rRNA gene, a locus associated with drug resistance, were designed based on the *Mycoplasma pneumoniae* M129 genome sequence (GenBank accession: NC_000912.1) (see Supplementary File 1, Table 1). Strain M129 is considered as a representative of one of the genetic types of *Mycoplasma pneumoniae* [35–37]. The reference sequence GCF_000027345.1 of *Mycoplasma pneumoniae* M129 was specified from two assemblies presented in the NCBI RefSEq database due to the highest completeness score by CheckM mentioned on the RefSeq assemblies pages.

The methodology for primer synthesis is detailed in the Supplementary File 2. Each PCR reaction mixture consisted of 7.5 µl Q5 Hot Start High-Fidelity 2X Master Mix (New England Biolabs, USA), 1 µl forward primer (10 mM), 1 µl reverse primer (10 mM), 0.5 µl H2O, and 5 µl DNA template.

The thermal cycling conditions were as follows: Stage 1: 98 °C for 1 min; Stage 2: 35 cycles of 98 °C for 10 s, 62 °C for 30 s, and 72 °C for 1 min; stage 3: 72 °C for 5 min.

Table 1 Main characteristics, biological data of patients with MPP and healthy control groups of children and adults. Data are N_x/N_{all} (%) of patients, mean ± standard deviation (SD)

Characteristic	N_x/N_{all} (%)
Children with MPP, all samples	
Total	193
Age (y)	11.94 (± 3.76)
Gender, N_x/N_{all} (%)	
Male	86/193 (44.6%)
Female	67/193 (34.7%)
Unknown	40/193 (20.7%)
Virial coinfection, N_x/N_{all} (%)	119/193 (62%)
MP with A2063G mutation, N_x/N_{all} (%)	36/90 (40%)
Control group 1	
Total	38
Age (y)	7.55 (± 3.24)
Gender, N_x/N_{all} (%)	
Male	21/38 (55.3%)
Female	17/38 (44.7%)
Unknown	0
Virial infection, N_x/N_{all} (%)	8/38 (21%)
MP with A2063G mutation, N_x/N_{all} (%)	0
Control group 2	
Total	72
Age (y)	35.75 (± 11.98)
Gender, N_x/N_{all} (%)	
Male	37/72 (45.8%)
Female	39/72 (54.2%)
Unknown	0
Virial infection, N_x/N_{all} (%)	39/72 (54%)
MP with A2063G mutation, N_x/N_{all} (%)	0

The expected size of the PCR products (900 base pairs, bp) was confirmed by visualizing the DNA fragments using agarose gel electrophoresis with ethidium bromide staining.

Amplification of the QRDR regions of the *parC* and *gyrA* genes (associated with fluoroquinolone resistance in bacteria)

Primers for amplifying the QRDR of the *parC* and *gyrA* genes were designed based on the reference *Mycoplasma pneumoniae* M129 genome sequence (NCBI accession: NC_000912.1) (see Supplementary File 1, Table 1). Each PCR reaction mixture contained: 7 µl PCR-mix-2 blue (Amplisens, Russia), 1 µl forward primer (10 mM), 1 µl reverse primer (10 mM), 1.5 µl 4.4 mM dNTP (Amplisens, Russia), 12.5 µl deionized water (H2O), 5 µl DNA template. The PCR program consisted of the following steps: initial denaturation at 95 °C for 2 min, 35 cycles of 10 s at 98 °C, 30 s at 62 °C, and 1 min at 72 °C, and final extension at 72 °C for 5 min.

The expected size of the PCR products (450 base pairs, bp) was confirmed by visualizing the DNA fragments using agarose gel electrophoresis with ethidium bromide staining.

PCR product purification and sequencing

The amplification products of the V region of the 23S rRNA gene and the QRDR regions of the *parC* and *gyrA* genes were purified using the ExS-Pure Enzymatic PCR Purification Kit (Nimagen, The Netherlands). Sanger sequencing was performed on the Honor1616 Genetic Analyser (Nanjing Weiyun Biotechnology Co., China) using the BrilliantDye Terminator Cycle Sequencing Kit v3.1 (Nimagen, Netherlands) for fluorescence-based cycle sequencing reactions.

If Sanger sequencing wasn't suitable due to the presence of multiple bands, we used Oxford Nanopore sequencing technology (ONT). For this, the PCR products were purified using MGIEasy DNA Clean Beads (MGI, China) and prepared for sequencing through adapter ligation with the SQK-LSK109 sequencing kit (Oxford Nanopore Technologies, UK) combined with the Native Barcoding Kit 96 (EXP-NBD112.96, Oxford Nanopore Technologies, UK), following the manufacturer's protocols. High-throughput sequencing was conducted on the PromethION device (Oxford Nanopore Technologies, UK) using an FLO-PRO002 flow cell with R9.4.1 chemistry.

Mycoplasma pneumoniae isolates cultivation

Twelve nasopharyngeal swabs from patients in Moscow diagnosed with *Mycoplasma pneumoniae* infections were collected in transport substrate (Hayflick broth without the addition of horse serum). The samples were transported from the hospital to the microbiology laboratory within three hours. Next, 0.2 ml of the sample in the transport substrate was inoculated into individual glass tubes with a two-phase (agar/broth) medium prepared as described in references [38, 39]. The tubes were incubated in an air incubator at 37 °C and monitored daily for two weeks for changes in color and appearance. After one week, growth was detected in three samples: MPsbm004 [4], MPsbm008 [8], and MPsbm010 [10].

The two-phase (agar/broth) medium composition included the following: 7 parts of 17.7 g/L brain–heart infusion (BHI) (Oxoid, USA), 2 parts of fetal calf serum (Himedia, India) 1 part of a 25% aqueous extract of baker's yeast (Bio Springer, France), 85% purified agar (PanReac AppliChem, Spain), Penicillin (1000 U/ml)

and thallium acetate (1:2000) as fungal and bacterial inhibitors.

The preparation of the two-phase medium involved two stages: (I) 1 ml of mycoplasma agar was poured into sterile 10-ml glass tubes and left for 30 min to allow the agar to solidify completely, (II): 2 ml of a liquid substrate (without agar), supplemented with 1% glucose and 0.004% phenol red, was added over the solidified agar.

Complete genomes sequencing of cultivated *Mycoplasma pneumoniae* isolates

The grown *M. pneumoniae* (MP) cells were transferred into sterile 1.5 ml tubes and centrifuged at 10,000 g for 10 min at 4 °C. The isolation of DNA was then performed by resuspending the pellet in 500 µl of a CTAB buffer composed of 2% CTAB (hexadecyltrimethylammonium bromide), 100 mM Tris–HCl (pH = 8), 20 mM EDTA, 1.4 M NaCl, and 0.1 mg/ml proteinase K (obtained from Thermo Fisher Scientific, USA). The suspension was incubated at 60 °C for 30 min. After incubation, 500 µl of chloroform was added, mixed thoroughly, and centrifuged at 10,000 g for 20 min at 4 °C. The aqueous phase was collected, and 500 µl of isopropanol along with 50 µl of 3 M sodium acetate were added. The mixture was incubated at −20 °C for 1 h, followed by centrifugation at 10,000 g for 20 min at 4 °C. The supernatant was discarded, and the pellet was washed twice with 50 µl of 80% ethanol. The pellet was air-dried for 10 min and then dissolved in 20 µl of deionized water.

To achieve the DNA concentration required for Oxford Nanopore Technologies (ONT) sequencing, whole-genome amplification (WGA) was performed. For this, 2.5 µl of the DNA was amplified using the REPLI-g Single Cell Kit (QIAGEN, the Netherlands), which employs the multiple strand displacement amplification method with ϕ29 DNA polymerase. The WGA products were purified using MGIEasy DNA Clean Beads (MGI, China) and eluted in 25 µl of deionized water. The purified PCR products were visualized on a 1% agarose gel (Supplementary File 1, Fig. 1).

The DNA concentration of the amplification products was measured using the Qubit dsDNA High Sensitivity kit (Thermo Fisher Scientific, USA) following the manufacturer's instructions. The final concentration of the samples was 770 ng/µl. Subsequently, 400 ng of each WGA product was treated with T7 endonuclease I (NEB, UK) according to the manufacturer's protocol.

For sequencing, library preparation was conducted using the Native Barcoding Kit 96 (EXP-NBD112.96, Oxford Nanopore Technologies, UK) and the Ligation Sequencing gDNA—Native Barcoding protocol (SQK-LSK109 with EXP-NBD112.96). Sequencing was performed on a PromethION platform (Oxford Nanopore Technologies, UK) using a FLO-PRO002 flow cell (chemistry R9.4.1). In total, the sequencing yielded 17.26 million reads and 20.27 GB of data.

Genome assembly and annotation

Genome assembly

Basecaling was performed using Guppy basecaller (v6.0.7) [40]. Reference based (NC_000912.1) assembly was performed with minimap2 (v2.27) [41], samtools (v1.19.2) [42] and medaka (v.1.11.3) [43]. Briefly, reads from both amplification approaches were merged and mapped onto the reference genome. A draft genome was generated from the alignment and subsequently polished using the original reads.

The quality of the assembly was assessed using QUAST (v5.2.0) [44]. For genome structure investigation, annotation was carried out with PGAP (2023–10-03.build7061) [45]. Relevant genomic features for further analysis were manually extracted from the generated GBK file.

Genome structure evaluation

The newly assembled genome was then aligned against the reference genome NC_000912.1 using the MUMmer package (v3.23) [46]. Nucleotide alignment was conducted with "NUCmer" (NUCleotide MUMmer version 3.1) using default parameters, while amino acid alignment was performed with "PROmer" (PROtein MUMmer version 3.07) with default settings.

MLST typing was carried out using the mlst toolkit (v. 2.23.0) by Seemann T, available online at https://github.com/tseemann/mlst, with default parameters.

To calculate alignment identity values, COORDS files generated by the "show-coords" utility (with the -k -r -l parameters) from the same package were utilized. Sequence alignments were visualized using the "mapview" utility (version 1.01) with default settings, while sequence similarity was illustrated using alignment dotplots generated by the "mummerplot" utility (version 3.5).

SNPs identification was performed using the "show-snps" utility (with the -C -r -l parameters) from the same package. The distribution of SNPs across sequence regions was analyzed using a custom script.

Antimicrobial resistance screening was conducted on the newly assembled genome using AMRFinderPlus (Software version: 3.12.8, Database version: 2024–05-02.2) [47] and by mapping the assembled genome against the MEGARes database of drug resistance sequences (v3.0.0) [48].

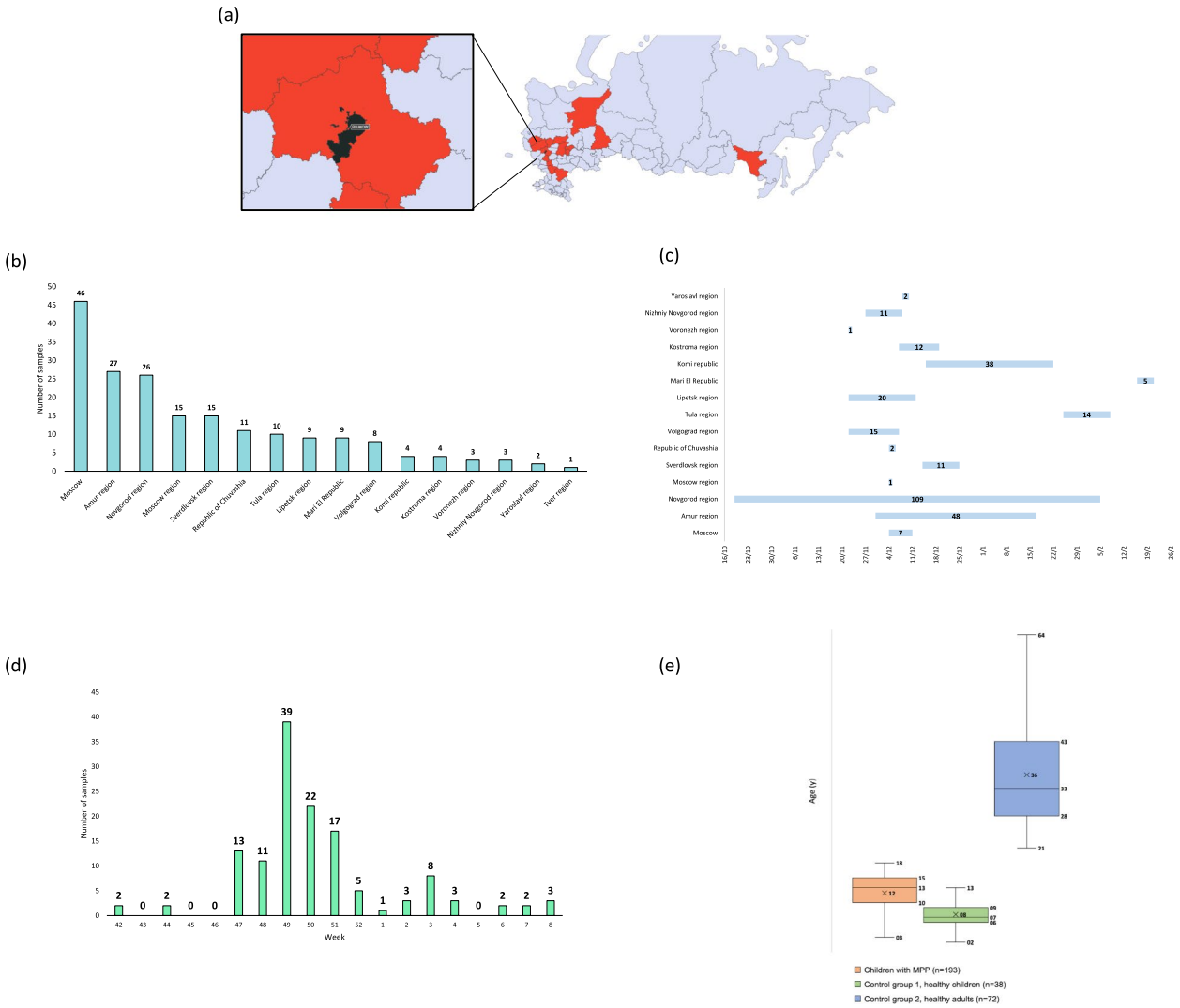

Fig. 1 Scheme of the distribution of sample collection regions across the Russian Federation (**a**) A map highlighting the regions where samples were collected, marked in red, with Moscow indicated in black; (**b**) The number of samples collected in each region; (**c**) The dates of sample collection for each region; (**d**) The number of samples collected per week; (**e**) A box plot showing the age distribution of participants in each group

Additionally, screening for extraneous viral and plasmid content was performed using the geNomad program set (v.1.8.0) [49].

Phylogenetic analysis

A dataset of 290 *M. pneumoniae* RefSeq genomes was retrieved using NCBI Datasets command-line tools [50] and combined with a novel genome. All genome annotations were converted to GFF format, including the genomic sequences, to facilitate subsequent pangenome analysis.

Core genes were identified and clusters visualized using Roary (v3.12.0) [51]. Roary was executed with the "-e" flag to generate a multi-FASTA alignment of core genes using PRANK, with a minimum blastp identity value of 95%. The summary of the pan-genome composition generated by Roary was visualized using the open-source Python script 'roary_plots.py' (available at https://github.com/sanger-pathogens/Roary/tree/master/contrib/roary_plots).

The alignment of core genes was used to construct a maximum likelihood (ML) phylogenetic tree with IQ-tree2 (v2.2.7), employing ModelFinder to select the best-fit model (TIM+F+I) [52, 53]. BioSample metadata was retrieved using edirect (v20.3) [54] and parsed using in-house Python scripts to enable descriptive phylogenetic tree visualization in iTOL [55].

Results

Analysis of the viral co-infections spectrum

From October 19, 2023, to February 21, 2024, nasopharyngeal swabs were collected from children diagnosed with pneumonia caused by *M. pneumoniae* in European Russia ($n=166$, including 60 samples from Moscow and the Moscow region) and the Far East of Russia ($n=27$, Amur region). The total number of samples obtained from children diagnosed with *M. pneumoniae* pneumonia (children with MPP) was 193 (see Supplementary File 1, Table 2).

As control groups, nasopharyngeal swabs were collected from 38 healthy children (Control group 1) and 72 healthy adults (Control group 2) in December 2023. The biological data and clinical characteristics of all collected samples are presented in Table 1, while the geographical locations and sampling details are illustrated in Fig. 1 (a-e).

Viral co-infection was detected in 119 out of 193 (62%) children with MPP, using real-time PCR. A variety of respiratory viruses were identified, including: hAdV; rhinovirus; seasonal coronaviruses (HKU1, OC43, 229E, NL-63); RSV types A and B; hBoV; MPV; HPIV types 1–4; SARS-CoV-2 (Fig. 2(a), Supplementary File 1 Table 2).The most frequently detected viral pathogens in children with MPP were human parainfluenza virus types 3 and 4 (HPIV-3 and HPIV-4), found in 35/193 (18%) and 51/193 (26.4%) patients, respectively. Other predominant viruses included SARS-CoV-2 (24/193, 12.4%), hAdV (8/193, 4%), and rhinovirus (8/193, 4%).

The control groups were tested for the same viral infections. Viral infections were detected in 8/38 (21%) of the healthy children and 39/72 (54%) of the healthy adults.

Among the most prevalent pathogens, coronaviruses were detected in healthy children: SARS-CoV-2 was identified in 6 out of 8 virus-positive children, while seasonal coronaviruses (HKU1, OC43, 229E, NL63) were found in 7 out of 8. In contrast, the most frequently identified pathogens in the healthy adult group were human parainfluenza viruses (HPIVs types 1–4), detected in 31 out of 72 (43%) individuals (Fig. 2(b, c); Supplementary File 1 Table 3; Supplementary File 1 Table 4). These findings suggest that the viruses most commonly co-infecting children with MPP are similar to those circulating among control group 1 (coronaviruses) and control group 2 (HPIVs).

It is important to note that a significant proportion (approximately 10–15%) of children with MPP, as well as healthy virus-positive children and adults, were coinfected with more than one respiratory virus. These findings are summarized in Table 2 and visualised in Fig. 2 (e).

The samples collected from all individuals in both control groups were screened for the presence of *M. pneumoniae* (MP) using real-time PCR. The results showed that 4 out of 38 control group 1 (10.5%) and 3 out of 72 control group 2 (4.1%) tested positive for MP. Importantly, none of these individuals developed pneumonia during the follow-up period.

We also attempted to analyze the region V of 23S rRNA gene and QRDRs (Quinolone Resistance-Determining Regions) of the *gyrA* and *parC* genes of *M. pneumoniae* in MP-positive individuals from both control groups. However, target amplification was unsuccessful due to low DNA concentrations, as reflected by high Ct-values (>30). These results are documented in Supplementary File 1, Tables 3 and 4.

To evaluate the prevalence of circulating viruses in the human population and to assess the environmental influence of viral circulation on the likelihood of viral co-infection in patients with MPP, a comparative analysis was conducted between children with MPP and control group 1. Since the samples from the control groups were collected in Moscow, a "Moscow subset" of samples from children with MPP from Moscow and the Moscow region (n=60) was selected for comparison.

The analysis revealed that the overall rate of viral infection was significantly higher in children with MPP (43/60, 71.6%) compared to control group 1 (8/38, 21%) and control group2 (39/72, 54%), indicating an increased risk of viral infection in children with MPP (Fig. 2 (d)).

Table 2 A number of viruses per sample in each group

Groups	Children with MPP	Cntrol group 1 (healthy children)	Control group 2 (healthy adults)
Sample number in the group	193	38	72
Coinfected with a single virus	90/193 (46.7%)	4/38 (10.5%)	31/72 (43%)
Coinfected with two viruses	24/193 (12.4%)	2/38 (5.3%)	7/72 (9.7%)
Coinfected with three viruses	3/193 (1.6%)	1/38 (2.6%)	1/72 (1.4%)
Coinfected with four viruses	1/193 (0.5%)	1/38 (2.6%)	-
Coinfected with seven viruses	1/193 (0.5%)	-	=
No viruses	74 (38.3%)	30(78.9%)	33 (45.8%)

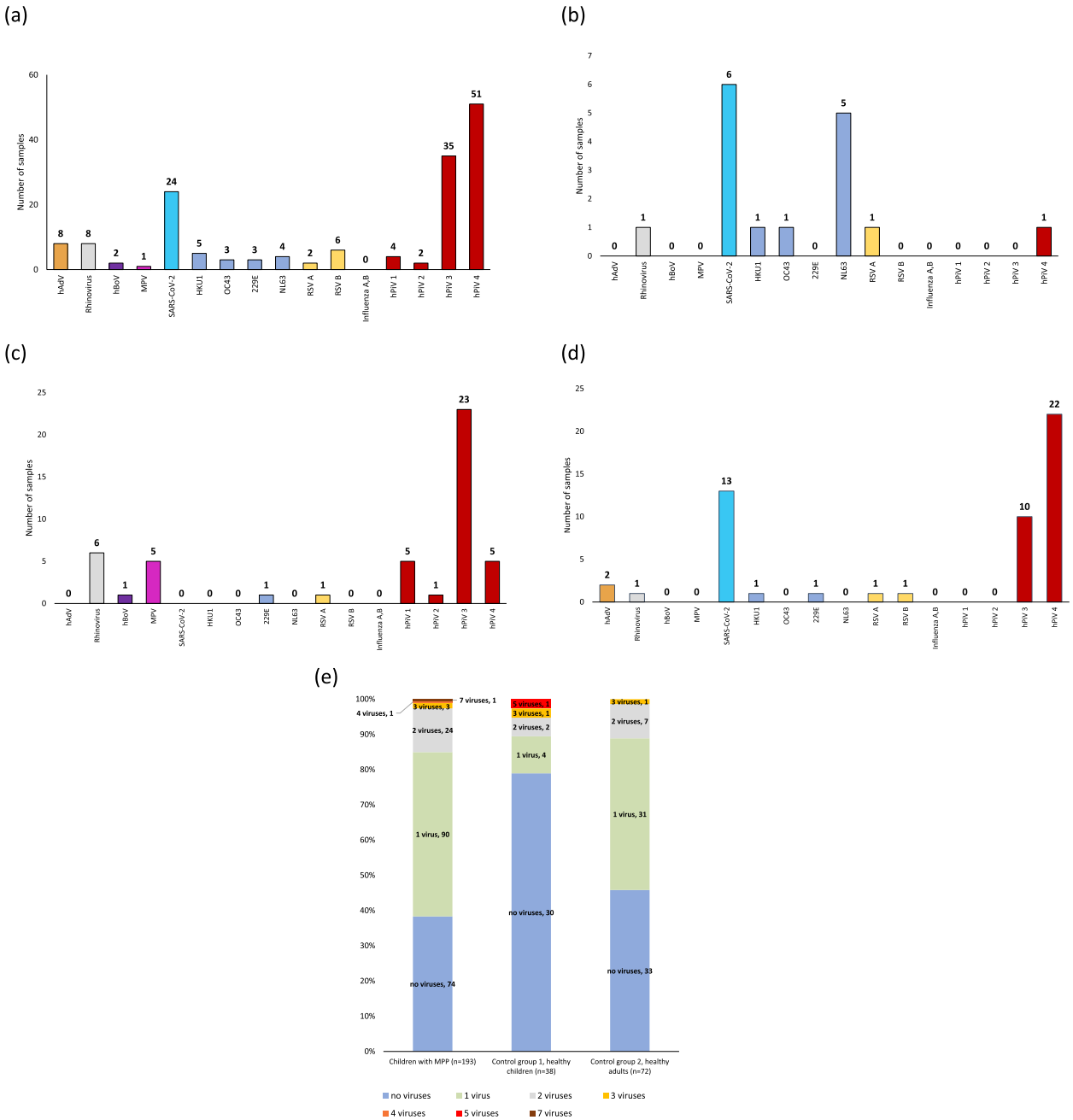

Fig. 2 The prevalence of respiratory viral infections. **a** Viral co-infections in children with MPP (Russian Federation); (**b**) Viral infections in healthy children (Control group 1); (**c**) Viral infections in healthy adults (Control group 2); (**d**) Viral co-infections in children with MPP (Moscow and Moscow region); (**e**) Number of viriuses per sample

Among individuals positive for viral infection, the rate of parainfluenza virus (HPIV) infection (primarily HPIV-3 and HPIV-4) was similar in children with MPP (32/60, 53.3%) and healthy adults (34/72, 47.2%). In contrast, the rate of HPIV infection in the healthy children group was significantly lower (1/38, 2.6%; $p < 0.002$). This finding suggests that the high prevalence of parainfluenza viruses in the general adult population likely contributes to the increased frequency of co-infections in MPP patients. The p-values for each analysis are provided in Table 3.

Table 3 Comparison of virial infections in children with MPP add healthy children (Fishers exact test)

Virus	*p*-value
hAdV	0.3724
Rhinovirus	1
hBoV	1
MPV	1
SARS-CoV-2	0.3294
HKU1	1
OC43	1.387
229E	0.8466
NL63	1.919
RSV A	1
RSV B	0.6122
Influenza A,B	1
HPIV 1	1
HPIV 2	1
HPIV 3	0.005383
HPIV 4	0.09588
HPIVs(1–4)	**0.00000003061***

**p*-value < 0,00294 (Bonferroni correction)

To assess the influence of geographic location and increased contact with individuals from China or Eastern Europe (due to proximity to the Chinese or western borders), a comparison of viral co-infection rates was conducted among subgroups of children diagnosed with MPP from European Russia (n = 166) and the Amur region (Far East, n = 27).

In contrast, HPIV-3 and HPIV-4 were the most prevalent co-infecting viruses in both regions. In European Russia, HPIV-3 was detected in 26/166 (15.6%) samples and HPIV-4 in 49/166 (29.5%). In the Far East, HPIV-3 was detected in 9/27 (33%) and HPIV-4 in 2/27 (7%).

These findings suggest that the prevalence of HPIV-3 and HPIV-4 can be explained by the widespread circulation of these viruses across a vast territory, extending from European Russia to the Far East. In contrast, the circulation of other respiratory viruses, such as SARS-CoV-2, appears to be more characteristic of localized areas. This highlights the potential role of population density and geographic factors in shaping the epidemiology of respiratory viral infections.

Macrolide resistance-associated mutations in MPP

Sequencing of the V region of the 23S rRNA gene (coordinates 1777–2661 bp) was performed for 90 samples from children with MPP. The results revealed that 36 patients (40%) carried MPP with the 2063 A/G mutation, which is associated with macrolide resistance. Additionally, two mutations with unknown clinical significance were identified: 2569 T/G in one patient (1.1%), 2590 T/G in another patient (1.1%).

No significant differences in macrolide resistance were observed between *M. pneumoniae* from European Russia and the Amur region. Specifically: the 2063 A/G mutation was detected in 5/14 (35.7%) samples from the Amur region and the same mutation was found in 31/76 (40.8%) samples from European Russia. These findings indicate that the prevalence of the 2063 A/G mutation is consistent across both geographic regions, suggesting a uniform distribution of macrolide resistance in MPP strains within the European Russia and Far East Russia human populations..

Fluoroquinolone resistance-associated mutations in MPP

The QRDR (Quinolone Resistance-Determining Region) of the *parC* gene (coordinates 73–503 bp) was sequenced for 45 samples, and the QRDR of the *gyrA* gene (coordinates 118–546 bp) was sequenced for 29 samples from children with MPP. No mutations were detected in the QRDR regions of either the *parC* or *gyrA* genes in any of the analyzed samples. This finding indicates the absence of quinolone resistance-associated mutations in these regions among the studied MPP cases.

Genome structure evaluation

M. pneumoniae from 12 clinical samples collected from Moscow patients (children with MPP) were incubated in culture media for a short period of 7–10 days before DNA extraction. The limited duration of the incubation phase was attributable to the experimental procedures being executed in the context of an investigation of an outbreak that occurred in December of 2023. As a result, a low bacterial load of *M. pneumoniae* was detected after the cultivation period, as confirmed by real-time PCR used for *M. pneumoniae* identification.

Among the 12 samples, 3 samples were successfully enriched with *M. pneumoniae*. To obtain a sufficient amount of DNA for sequencing, the DNA extracted from these 3 samples was subjected to whole genome amplification (WGA). This step was necessary to overcome the limitations posed by the low bacterial load and to enable downstream genomic analyses.

The products of WGA were then subjected to ONT sequencing, with a subsequent reference-based genome assembly, as outlined in the Materials and Methods section. For one of the three samples (MPsbm004), the assembly yielded a whole genome with depth coverage over 100X (Genbank acc. num. CP155805.1), while the assembly of two other samples (MPsbm008 and MPsbm010) yielded only contigs of varying length and lower depth coverage. The assembled genome CP155805.1 and contigs from samples MPsbm008 and

MPsbm010 were aligned to the reference *M. pneumoniae* M129 genome (NC_000912.1, GCF_000027345.1) with the MUMmer package [46] (see Fig. 2 (a)-(c) in the Supporting Information). The whole genome of sample MPsbm004 comprised 100% length coverage, while 99% and 79% length coverage was obtained for the genomic sequences of samples MPsbm008 and MPsbm010, respectively. However, the latter two genomic sequences showed very uneven coverage of the assembled regions, ranging from 1 to 150X. This resulted in their exclusion from further analysis.

The whole genome sequence of sample MPsbm004 (hereafter referred to as the novel genome, CP155805.1) that was selected for further detailed evaluation and phylogenetic analysis. The GC-content of the novel *M. pneumoniae* genome is about 40% within 816,452 base pairs (bp), which corresponds to 880 genomic features. Utilizing in-silico multi-locus sequence typing (MLST) typing against conventional PubMLST typing schemes as described in the Materials and Methods section, the genome CP155805.1 was classified as *M. pneumoniae* sequence type 3 with the following allelic profile: *ppa*(1), *pgm*(2), *gyrB*(1), *gmk*(1), *glyA*(1), *atpA*(3), *arcC*(1), *adk*(1).

A novel *M. pneumoniae* genome was aligned against the reference NC_000912.1 (GCF_000027345.1) using the NUCmer program [46], as outlined in the Materials and Methods section. This alignment revealed a 99.96% similarity for the primary alignment cluster. However, when considering secondary alignment clusters, the similarity reduces to 83% for certain alignments. The majority of these clusters refer to the regions of the *adhesin P1* gene and its pseudo-homologues, with the primary cluster still aligning at this region at a high score. Short non-matching alignment regions, including rearrangement or inversion events, were observed in the genome alignments. However, none of the extended ones were observed (Supplementary File 1, Fig. 2 (a)-(c)). An additional alignment of the novel genome CP155805.1 against the reference M129 *M. pneumoniae* genome (NC_000912.1) was conducted utilizing the MUMmer program [46], resulting in the identification of 447 single-nucleotide polymorphisms (SNPs), with an average of 5.5 SNPs per 10 kilobases for the 10-kilobase sliding window calculated manually from MUMmer results (Supplementary File 1, Fig. 3). The highest mutation rate was observed at the region from 410 to 420 kb, which corresponds to the MPN_RS01915 gene (409,562–410863 bp) in the coordinates of the reference *M. pneumoniae* M129 genome. The MPN_RS01915 gene protein product (WP_015344903.1) has been found to be associated with DNA modification (GO:0006304) and DNA binding (GO:0003677) functions. The extended SNP region represents a truncated 'ELSA' motif corresponding to the MgtE intracellular N-domain of the reference protein WP_015344903.1. This domain is reported as corresponding to magnesium transporters, but further biochemical studies are required to investigate the influence of this amino acid deletion.

No acquired resistance genes to various antibiotics were detected either for the genome or annotated proteins with AMRFinderPlus [47], none of viral or plasmid content was detected with geNomad [50]. MEGARes [48] usage revealed mutations required to be additionally confirmed for macrolide resistance which is described under the relevant section.

Phylogenetic analysis

The phylogenetic analysis was conducted on 290 complete *M. pneumoniae* genomes with supporting metadata obtained from RefSeq, as detailed in the Materials and Methods section. The Pangenome was constructed using Roary [51] with a total of 291 genomes, which included RefSeq genomes and the genome CP155805.1 obtained in this study. The core genes analysis revealed 167 genes shared by almost every ($\geq$ 288) genome included in the study out of a total of 789 genes. In contrast, Meng Xu and colleagues observed 624 core genes in a pangenome of 937 genes [56]. This discrepancy can be attributed to the augmented number of samples utilised in our study in comparison with the number of genomic sequences used by our colleagues (87 samples). This increased number of genomic sequences resulted in an increased quantity of unmatching genes at a constant gene homology level. Furthermore, we observed enhanced pangenome resolution and core gene identification with PGAP [45] annotations in comparison to Prokka [57] annotations, which is recommended by Roary authors. Conversely, Prokka usage has been observed to result in interrupted protein sequences when utilised with the "Bacteria" and "Mycoplasmoides" options for "Kingdom" and "Genus", respectively.

A maximum likelihood phylogenetic tree build on the pangenome core genes alignment reveals distinct clades correlating with results obtained by Yu-Chia Hsieh and colleagues [58]. Both of the approaches for the phylogenetic tree construction — on binary absence-presence or core genes alignment — place the novel *M. pneumoniae* genome to the clade 1 (Fig. 3).

While one complete novel genome CP155805.1 from sample MPsbm004 was included in pangenome analysis, assemblies from two other samples (MPsbm008 and MPsbm010) were too fragmented in terms of genome continuity to be included in pangenome to prevent results downshifting. Therefore we characterised two partial genomes assemblies from two other samples (MPsbm008 and MPsbm010) through comparative analysis of chosen

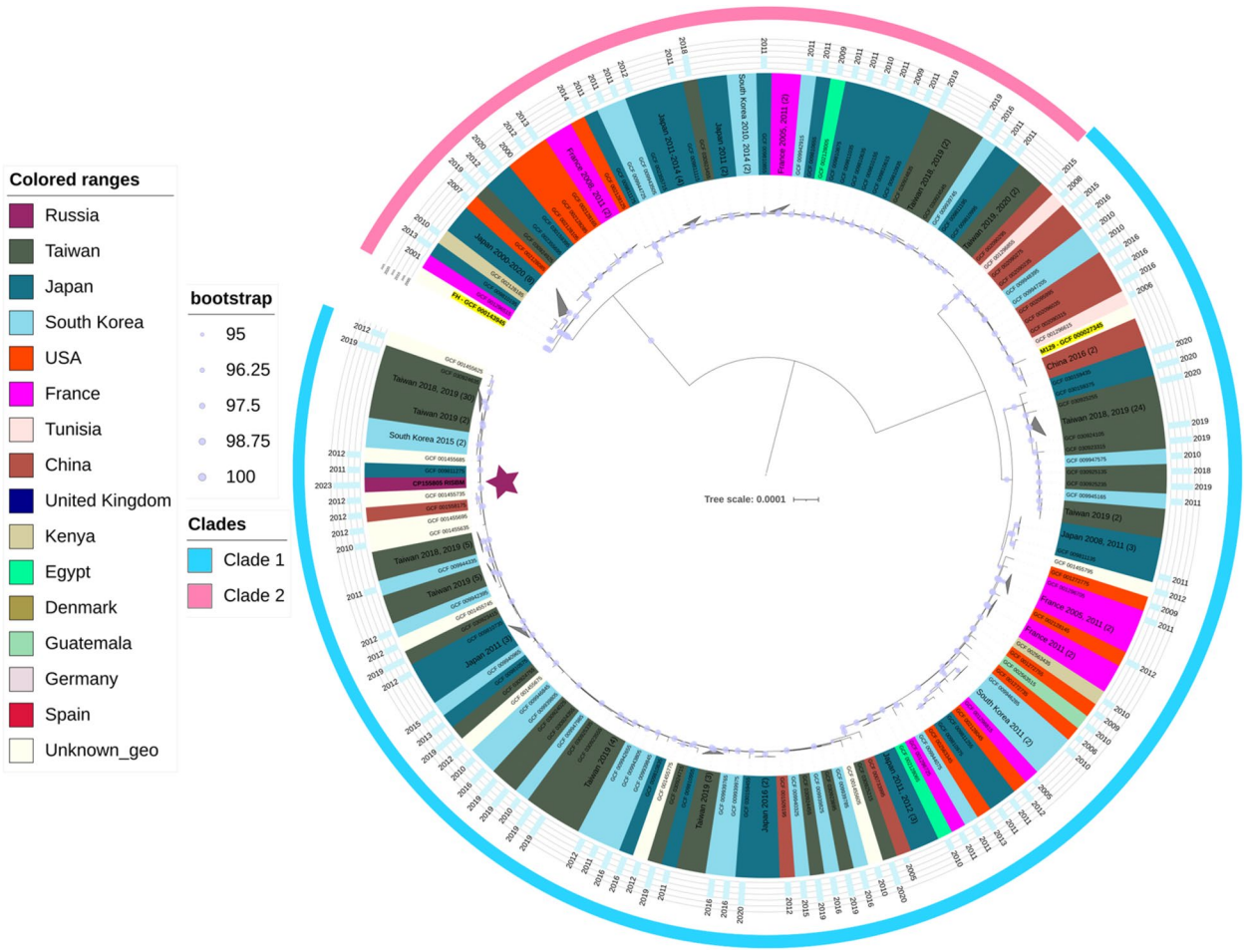

Fig. 3 Phylogenetic tree using core genes alignment with the metadata specified. Purple star corresponds to the novel *M. pneumoniae* genome

genomic features. To investigate the placement of these samples, adhesin protein coding sequences (*mgpA* gene) were manually extracted from the contigs and aligned with the *mgpA* of the novel genome CP155805.1 using a pairwise comparison. One of the samples (MPsbm008) contained a fourfold repeated "ATG" motif at the nucleotide position 1935 and a deletion C2905 in the coordinates of the novel genome adhesin gene. This sample may be assigned to the P1 type 1 clade. The other sample (MPsbm010), which exhibited the highest degree of fragmentary and the lowest level of coverage, yielded a multitude of mutations in the adhesin nucleotide sequence. However, these were not considered due to the low confidence of the overall sequence.

Discussion

In this study we report on the increase of MPP in children from different regions of Russia, 2023–2024. We analyzed nasopharyngeal swabs from 193 patients diagnosed with MPP from multiple hospitals. Most of the patients (82%) were school-aged patients, i.e. 7–17 years. Prior to 2023, the last reports on MP characterisation in children in Russia refer to 2018 [59] and mentioned in 2023 in Rachina et al. [16], but several studies worldwide have shown that mycoplasma infections are more common in school-aged children than in children under 6 years of age [60–63].

Viral co-infection with *M. pneumoniae* is often studied in the literature as it may influence the severity of the course and the effectiveness of treatment [64]. In children, several previous studies suggest that patients with co-infections account for 30–52% of *M. pneumoniae* infections [65–67] and that mixed viral-bacterial aetiology is common in children with lower respiratory tract infections [68]. In the current study the co-infection rate of *M. pneumoniae* and viral pathogen was 62%. The most common viral pathogens among patients with MPP were HPIVs (1-4) and SARS-CoV-2. It should be noted that in healthy adults (whose sample was sufficient for statistical analysis), HPIVs (1-4) and a variety of coronaviruses

were also predominant. In our opinion, in the fall-winter period 2023–2024 in Russia (at least in Moscow) in the population actively circulated viral strains that did not cause serious symptoms of acute respiratory viral infections in adults, but caused a complications when combined with mycoplasma infection in children, or—on the contrary—mycoplasma infection caused a complications when combined with viral infection. This hypothesis is supported by the fact that mycoplasma has been detected in 4/38 healthy children. Two of them were from the same family, one of them had 5 viruses in addition to mycoplasma infection and the other one had three additional viruses.

Previously, it has been reported that MP can co-infect a host along with bacteria and viruses, the co-infection rate can reach 52% [69] and compared with mono-infection, MP co-infection causes serious clinical symptoms and the clinical manifestations are more diverse [69, 70].

According to several studies by scientists in China, different viral pathogens were prevalent in patients with MPP in different years before the COVID-19 pandemic. For example, influenza type B was identified in 2010–2014 [20], hBoV in 2011–2016 [23], hAdV, rhinovirus, and HPIV 3 in 2016–2019 [18, 19, 21].The frequency of viral co-infections increased in the post-pandemic period. The most frequent viral pathogens in patients diagnosed with MP in China were AdV, RSV, while our study reveals the HPIVs and SARS-CoV-2 predominant pathogens during the 2023–2024 autumn–winter season in Russia, with no significant association observed between these pathogens and mycoplasma infection [71–73]. It is hypothesized that HPIVs and SARS-CoV-2 were the predominant pathogens during the 2023–2024 autumn–winter season in Russia, with no significant association observed between these pathogens and mycoplasma infection.

The important aspect affecting the effectiveness of treatment of MPP is resistance to macrolides, which has been rising worldwide since the 2000s [2, 74, 75]. We found that the rate of MP resistance to macrolides (MRMP) was 40.8% in European Russia and 35.7% in the Far East of Russia (Amur region), in the fall-winter of 2023–2024. These rates are higher compared to the MRMP rate in European countries (0–30%) [76] and the USA where the mutation rate has been below 30% since the 2010s [77, 78]. The MRMP rate in the Amur region of Russia (which is located near China) was definitely lower than those reported in other studies in China where the rates range from almost 70–90% during last ten years [79, 80], and in Korea, where the MP resistance rate was ~ 70% from May 2019 to April 2020 [17]. Excessive exposure to macrolides and antimicrobial selection pressure may explain the relatively high mutation rate in China [81]. In Korea, MRMP has shown a significant increasing trend, from 4 to 78% between 2008 and 2017 [82]. From 2019–2020, the rate of MRMP pneumonia in Korea continued to rise, with an overall macrolide resistance rate −78% [83]. A study from Japan reported a decline of resistance rate from 81.6% detected in 2012 to 43.6% in 2015, which correlates with the decrease in the use of oral macrolides [84]. It is possible that MRMP rates in different countries vary from year to year or between studies, but in the fall-winter of 2023–2024, we did not see a worrisome increase in MRMP rates in Russian patients with MPP.

In healthy children 10.5% and in healthy adults 4.1% were found to be positive for MP. No pneumonia or other respiratory symptoms were observed in the healthy group when followed up, which means that these patients are considered to be asymptomatic carriers. The existence of asymptomatic carriage of *M. pneumoniae* has been established previously. Recent studies indicate that high rates of healthy children carry *M. pneumoniae* in the upper respiratory tract and that current diagnostic PCR or serology cannot discriminate between *M. pneumoniae* symptomatic infection and carriage [85, 86]. Furthermore, clinical symptoms and radiological features are not always specific only for MP infection [86]. As a result, patients may be unnecessarily treated with antibiotics against *M. pneumoniae*, which may contribute to the spread of resistant forms of *M. pneumoniae*.

One limitation of the PCR diagnostic method is the potential for cross-contamination between samples. In the current study, PCR testing was performed in the laboratory by experienced staff according to standardized guidelines, however, the possibility of cross-contamination cannot be entirely ruled out. All experiments were performed in strict accordance with the protocols provided by the kit manufacturers, including the use of positive and negative controls. Nevertheless, for samples with very high Ct values, the risk of contamination occurring between the patient's arrival at the hospital and the collection of samples from the patient cannot be excluded.

Since these bacteria are very demanding on the nutrient medium due to genome reduction and the absence of many metabolic pathways, the cultivation of clinical isolates of mycoplasma is quite a complex task. Due to long-term persistence in the host organism, the metabolism of mycoplasmas adapts to the conditions of metabolite flows in the eukaryotic cell. And when such bacteria are transferrred to in vitro conditions, only a small percentage of bacteria can reconfigure their metabolism and adapt to cultivation in laboratory conditions. Moreover, suitable transport of the clinical specimens to the laboratory is crucial [87]. Thus, we have sequenced and assembled for the first time the one complete MP genome (CP155805.1) isolated

from a Russian patient. We have obtained incomplete MP genomes from two other grown isolates, the data of which are not presented in this article. The result of phylogenetic analysis for the assembled CP155805.1 genome demonstrates that the sequence obtained from Russia clusters with sequences from clade 1. Most of the complete MP genomes in this clade are represented by sequences from southeast Asia, with few sequences from patients of Europe, Africa and South America. The most of the closest genomes within the gene presence-absence metrics place the novel MP to the recent samples from Asian countries. But we should view the predominance of Asia sequences in clade 1 with caution, as the predominant number of MP complete genomes are from Asian samples, which shifts the pangenome sampling groups and results.

Russian MP strain (CP155805.1) was categorized as type P1 type 1. The prevalence of P1 type 1 (85.7%) was observed in Beijing, China during the MPP outbreak in June 2023 [10]. The Asian clade placement results should be viewed with caution, as the preponderance of MP complete genomes are from Asian samples, which shifts the pangenome sampling groups and results. Nevertheless, most of the closest genomes within the gene presence-absence metrics place the novel MPP in the most recent samples from Asian countries.

Conclusion

Several regions in European Russia and the Far East (Amur region) have experienced the outbreak of *Mycoplasma pneumoniae* infection in school-aged children, fall-winter 2023–2024. In children with MPP, 62% of cases are demonstrated co-infection of respiratory viruses. Co-infection of MP with HPIVs and SARS-CoV-2 viruses were the most cases (47.7% and 12.4% respectively) in patients with MPP and the same viruses were actively circulating in the population among healthy children and adults in December 2023. The rate of MRMP was 40.8% in European Russia and in 35.7% Amur region (The Far East). Phylogenetic analysis showed the obtained MP genome related to P1 type 1.

Supplementary Information

The online version contains supplementary material available at https://doi.org/10.1186/s12879-025-10712-0.

Supplementary Material 1.

Supplementary Material 2.

Acknowledgements

The authors acknowledge the staff of the Centers for Hygiene and Epidemiology in Amur region, Republic of Chuvashia, Komi Republic, Kostroma region, Lipetsk region, Mari El Republic, Novgorod region, Nizhny Novgorod region, Moscow, Moscow region, Sverdlovsk region, Tula region, Volgograd region, Voronezh region, Yaroslavl region for participating in the study and providing the samples.

Authors' contributions

EK: Data curation, Methodology, Writing – original draft, Writing – review & editing. IR: Data curation, Methodology, Writing – original draft, Writing – review & editing. IC: Data curation, Methodology, Writing – original draft, Writing – review & editing. AL: Methodology, Writing – review & editing. AK: Methodology, Writing – original draft, Writing – review & editing. IB: Writing – review & editing. JK: Methodology, Writing – original draft, Writing – review & editing. OF: Methodology, Writing – original draft, Writing – review & editing. DE: Data curation, Writing – original draft, Writing – review & editing. AS: Writing – original draft, Writing – review & editing. DM: Writing – original draft, Writing – review & editing. VG: Conceptualization, Data curation, Writing – review & editing AS: Methodology, Conceptualization, Data curation, Writing – original draft, Writing – review & editing.

Funding

This study was supported by state project (No. 12203090069–4).

Data availability

Sequences of V region of 23 s rRNA gene were deposited in Genbank NCBI under accession numbers: PQ014808-PQ014812, PQ113738, PQ014814, PQ014815, PQ014810, PQ014817, PQ014818, PQ014811, PQ014812, PQ014813, PQ113739, PQ014823, PQ014814, PQ014815, PQ014816, PQ014817, PQ113740, PQ014818, PQ014830, PQ114607, PQ014819-PQ014821, PQ114608, PQ014822, PQ114613, PQ014835, PQ014836, PQ014837, PQ014838, PQ114609, PQ014839, PQ014840, PQ014841, PQ014842, PQ014820, PQ014821, PQ014822, PQ014847, PQ014823, PQ014849, PQ014850, PQ014851, PQ014852, PQ014853, PQ014854, PQ014824, PQ014825, PQ014857, PQ014858, PQ014859, PQ014826, PQ014827, PQ014828, PQ014827, PQ014864, PQ014865, PQ014828, PQ014867, PQ014868, PQ114590, PQ014870, PQ014830, PQ014831, PQ014832, PQ014833, PQ014835, PQ014836, PQ014837, PQ014838, PQ014839, PQ014840, PQ014841, PQ014842, PQ014843, PQ014844, PQ014845, PQ014846, PQ014847, PQ014848, PQ014849, PQ113741, PQ114594, PQ014850, PQ114593, PQ014851, PQ014852, PQ114597, PQ014853, PQ014854, PQ114595, PQ014855, PQ114598, PQ014856, PQ114599, PQ014857, PQ114610, PQ014858, PQ014859, PQ114605, PQ014860, PQ114606, PQ014861, PQ014862, PQ114612, PQ114604, PQ014863, PQ113742, PQ014864, PQ114611, PQ114600, PQ114601, PQ114602, PQ114603, PQ014865, PQ014866, PQ014867, PQ014867, PQ014868, PQ014869, PQ014869, PQ014870, PQ014871, PQ014872, PQ014873, PQ014874, PQ014875, PQ014876, PQ014877, PQ113743, PQ014878, PQ114592, PQ014879, PQ014880, PQ014881, PQ014882, PQ114591, PQ014883. Whole genome sequence was deposited in Genbank NCBI under accession number CP155805.1 The sequences of the QRDR locus of the parC and gyrA genes: have been deposited in the Genbank NCBI under the accession numbers PQ374448- PQ374481.

Whole genome sequence was deposited in Genbank NCBI under accession number CP155805.1

The sequences of the QRDR locus of the parC and gyrA genes: have been deposited in the Genbank NCBI under the accession numbers PQ374448- PQ374481.

Declarations

Ethics approval and consent to participate

This study was approved by the Ethics Committee of the Research Institute of Systems Biology and Medicine, Federal Service for Consumer Rights Protection and Human Well-being Surveillance, Moscow, Russia (Protocol №3 (19.08.2024)) in accordance with the declaration of Helsinki and International ethical guidelines for biomedical research involving human subjects. Written informed consent to participate was obtained from all enrolled patients (or their parent or legal guardian in the case of children under 16).

Consent for publication

As the data obtained from swab analysis is anonymized and the study is performed without any personal identifiers, it was determined that obtaining informed consent for publication was unnecessary.

Competing interests
The authors declare no competing interests.

Author details
[1]Scientific Research Institute for Systems Biology and Medicine, Federal Service on Consumer Rights Protection and Human Well-Being Surveillance, Moscow, Russia. [2]Moscow Institute of Physics and Technology National Research University, Dolgoprudny, Moscow, Russia. [3]Federal State Budgetary Educational Institution of Further Professional Education "Russian Medical Academy of Continuous Professional Education" of the Ministry of Healthcare of the Russian Federation, Moscow, Russia. [4]Vavilov Institute of General Genetics, Russian Academy of Sciences, Moscow, Russia.

Received: 1 October 2024 Accepted: 24 February 2025
Published online: 15 March 2025

References

1. Waites KB, Talkington DF. Mycoplasma pneumoniae and its role as a human pathogen. Clin Microbiol Rev. 2004;17(4):697–728, table of contents.
2. Waites KB, Xiao L, Liu Y, Balish MF, Atkinson TP. Mycoplasma pneumoniae from the Respiratory Tract and Beyond. Clin Microbiol Rev. 2017;30(3):747–809.
3. Zhao H, Li S, Cao L, Yuan Y, Xue G, Feng Y, et al. Surveillance of Mycoplasma pneumonia einfection among children in Beijing from 2007 to 2012. Chin Med J. 2014;127(7):1244.
4. Cheng Y, Cheng Y, Dai S, Hou D, Ge M, Zhang Y, et al. The Prevalence of Mycoplasma Pneumoniae Among Children in Beijing Before and During the COVID-19 Pandemic. Front Cell Infect Microbiol. 2022;12.
5. Onozuka D, Hashizume M, Hagihara A. Impact of weather factors on Mycoplasma pneumoniae pneumonia. Thorax. 2009;64(6):507–11.
6. Onozuka D, Chaves LF. Climate variability and nonstationary dynamics of Mycoplasma pneumoniae pneumonia in Japan. PLoS ONE. 2014;9(4):e95447.
7. Yamazaki T, Kenri T. Epidemiology of Mycoplasma pneumoniae Infections in Japan and Therapeutic Strategies for Macrolide-Resistant M. pneumoniae. Front Microbiol. 2016;7:693.
8. Meyer Sauteur PM, Beeton ML, Uldum SA, Bossuyt N, Vermeulen M, Loens K, et al. Mycoplasma pneumoniae detections before and during the COVID-19 pandemic: results of a global survey, 2017 to 2021. Euro Surveill. 2022;27(19):2100746.
9. Meyer Sauteur PM, Beeton ML, European Society of Clinical Microbiology and Infectious Diseases (ESCMID) Study Group for Mycoplasma and Chlamydia Infections (ESGMAC), and the ESGMAC Mycoplasma pneumoniae Surveillance (MAPS) study group. Mycoplasma pneumoniae: delayed re-emergence after COVID-19 pandemic restrictions. Lancet Microbe. 2024;5(2):e100–1.
10. Yan C, Xue GH, Zhao HQ, Feng YL, Cui JH, Yuan J. Current status of Mycoplasma pneumoniae infection in China. World Journal of Pediatrics. 2024;20(1):1.
11. Zhang XB, He W, Gui YH, Lu Q, Yin Y, Zhang JH, et al. Current Mycoplasma pneumoniae epidemic among children in Shanghai: unusual pneumonia caused by usual pathogen. World J Pediatr. 2024;20(1):5–10.
12. Schweon SJ. Global reemergence of Mycoplasma pneumoniae. Nursing2024. 2024;54(5):11.
13. Edouard S, Boughammoura H, Colson P, La Scola B, Fournier PE, Fenollar F. Large-Scale Outbreak of Mycoplasma pneumoniae Infection, Marseille, France, 2023–2024. Emerg Infect Dis. 2024;30(7):1481–4.
14. Bolluyt DC, Euser SM, Souverein D, van Rossum AM, Kalpoe J, van Westreenen M, et al. Increased incidence of Mycoplasma pneumoniae infections and hospital admissions in the Netherlands, November to December 2023. Euro Surveill. 2024;29(4):2300724.
15. Urbieta AD, Barbeito Castiñeiras G, Rivero Calle I, Pardo Seco J, Rodríguez Tenreiro C, Suárez Camacho R, et al. Mycoplasma pneumoniae at the rise not only in China: rapid increase of Mycoplasma pneumoniae cases also in Spain. Emerg Microbes Infect. 2024Dec;13(1):2332680.
16. Rachina SA, Kupryushina OA, Yasneva AS, Volosovtsova ES, Strelkova DA, Avdeev SN, Frangu RK, Merzhoeva ZM, Samokhina AS, Eryshova DS, Tikhonova MA, Yatsyshina SB. What Do We Know about Mycoplasmal Pneumonia? Pract Pulmonol. 2023;3:20–32.
17. Shin S, Koo S, Yang YJ, Lim HJ. Characteristics of the Mycoplasma pneumoniae Epidemic from 2019 to 2020 in Korea: Macrolide Resistance and Co-Infection Trends. Antibiotics (Basel). 2023;12(11):1623.
18. Zhou Y, Wang J, Chen W, Shen N, Tao Y, Zhao R, et al. Impact of viral coinfection and macrolide-resistant mycoplasma infection in children with refractory Mycoplasma pneumoniae pneumonia. BMC Infect Dis. 2020;20:633.
19. Li F, Zhang Y, Shi P, Cao L, Su L, Fu P, et al. Mycoplasma pneumoniae and Adenovirus Coinfection Cause Pediatric Severe Community-Acquired Pneumonia. Microbiol Spectr. 2022;10(2):e00026-e122.
20. Song Q, Xu BP, Shen KL. Effects of bacterial and viral co-infections of mycoplasma pneumoniae pneumonia in children: analysis report from Beijing Children's Hospital between 2010 and 2014. Int J Clin Exp Med. 2015;8(9):15666–74.
21. Zhao M chuan, Wang L, Qiu F zhou, Zhao L, Guo W wei, Yang S, et al. Impact and clinical profiles of Mycoplasma pneumoniae co-detection in childhood community-acquired pneumonia. BMC Infect Dis. 2019;19:835.
22. Chiu CY, Chen CJ, Wong KS, Tsai MH, Chiu CH, Huang YC. Impact of bacterial and viral coinfection on mycoplasmal pneumonia in childhood community-acquired pneumonia. J Microbiol Immunol Infect. 2015;48(1):51–6.
23. Zhang X, Chen Z, Gu W, Ji W, Wang Y, Hao C, et al. Viral and bacterial coinfection in hospitalised children with refractory Mycoplasma pneumoniae pneumonia. Epidemiol Infect. 2018;146(11):1384–8.
24. Pereyre S, Goret J, Bébéar C. Mycoplasma pneumoniae: Current Knowledge on Macrolide Resistance and Treatment. Front Microbiol. 2016;7:974.
25. Tsai TA, Tsai CK, Kuo KC, Yu HR. Rational stepwise approach for Mycoplasma pneumoniae pneumonia in children. J Microbiol Immunol Infect. 2021;54(4):557–65.
26. Oishi T, Ouchi K. Recent Trends in the Epidemiology, Diagnosis, and Treatment of Macrolide-Resistant Mycoplasma pneumoniae. J Clin Med. 2022;11(7):1782.
27. Bébéar CM, Pereyre S. Mechanisms of drug resistance in Mycoplasma pneumoniae. Curr Drug Targets Infect Disord. 2005;5(3):263–71.
28. Bébéar C, Pereyre S, Peuchant O. Mycoplasma pneumoniae: susceptibility and resistance to antibiotics. Future Microbiol. 2011;6(4):423–31.
29. Principi N, Esposito S. Macrolide-resistant Mycoplasma pneumoniae: its role in respiratory infection. J Antimicrob Chemother. 2013;68(3):506–11.
30. Sulyok KM, Kreizinger Z, Wehmann E, Lysnyansky I, Bányai K, Marton S, et al. Mutations Associated with Decreased Susceptibility to Seven Antimicrobial Families in Field and Laboratory-Derived Mycoplasma bovis Strains. Antimicrob Agents Chemother. 2017;61(2):e01983-e2016.
31. Gautier-Bouchardon AV, Reinhardt AK, Kobisch M, Kempf I. In vitro development of resistance to enrofloxacin, erythromycin, tylosin, tiamulin and oxytetracycline in *Mycoplasma gallisepticum*, *Mycoplasma iowae* and *Mycoplasma synoviae*. Vet Microbiol. 2002;88(1):47–58.
32. Gruson D, Pereyre S, Renaudin H, Charron A, Bébéar C, Bébéar CM. In vitro development of resistance to six and four fluoroquinolones in Mycoplasma pneumoniae and Mycoplasma hominis, respectively. Antimicrob Agents Chemother. 2005;49(3):1190–3.
33. Yoshida H, Bogaki M, Nakamura M, Nakamura S. Quinolone resistance-determining region in the DNA gyrase gyrA gene of Escherichia coli. Antimicrob Agents Chemother. 1990;34(6):1271–2.
34. Bébéar CM, Renaudin H, Charron A, Clerc M, Pereyre S, Bébéar C. DNA gyrase and topoisomerase IV mutations in clinical isolates of Ureaplasma spp. and Mycoplasma hominis resistant to fluoroquinolones. Antimicrob Agents Chemother. 2003;47(10):3323–5.
35. Kenri T, Yamazaki T, Ohya H, Jinnai M, Oda Y, Asai S, et al. Genotyping of Mycoplasma pneumoniae strains isolated in Japan during 2019 and 2020: spread of p1 gene type 2c and 2j variant strains. Front Microbiol. 2023;14.
36. Edelstein I, Rachina S, Touati A, Kozlov R, Henin N, Bébéar C, et al. Mycoplasma pneumoniae Monoclonal P1 Type 2c Outbreak, Russia, 2013. Emerg Infect Dis. 2016;22(2):348–50.
37. Liu Y, Ye X, Zhang H, Xu X, Li W, Zhu D, et al. Antimicrobial Susceptibility of Mycoplasma pneumoniae Isolates and Molecular Analysis of Macrolide-Resistant Strains from Shanghai. China Antimicrobial Agents and Chemotherapy. 2009;53(5):2160–2.

38. Chanock RM, Hayflick L, Barile MF. Growth on artificial medium of an agent associated with atypical pneumonia and its identification as a pplo. Proc Natl Acad Sci. 1962;48(1):41–9.
39. Hayflick L, Chanock RM. Mycoplasma Species of Man. Bacteriol Rev. 1965;29(2):185–221.
40. Wick RR, Judd LM, Holt KE. Performance of neural network basecalling tools for Oxford Nanopore sequencing. Genome Biol. 2019;20(1):129.
41. Li H. Minimap2: pairwise alignment for nucleotide sequences. Bioinformatics. 2018;34(18):3094–100.
42. Danecek P, Bonfield JK, Liddle J, Marshall J, Ohan V, Pollard MO, et al. Twelve years of SAMtools and BCFtools. Gigascience. 2021;10(2):giab008.
43. Medaka 2018- Oxford Nanopore Technologies Ltd, available online, https://github.com/nanoporetech/medaka (accessed 1 March 2024).
44. Gurevich A, Saveliev V, Vyahhi N, Tesler G. QUAST: quality assessment tool for genome assemblies. Bioinformatics. 2013;29(8):1072–5.
45. Li W, O'Neill KR, Haft DH, DiCuccio M, Chetvernin V, Badretdin A, et al. RefSeq: expanding the Prokaryotic Genome Annotation Pipeline reach with protein family model curation. Nucleic Acids Res. 2021;49(D1):D1020–8.
46. Kurtz S, Phillippy A, Delcher AL, Smoot M, Shumway M, Antonescu C, et al. Versatile and open software for comparing large genomes. Genome Biol. 2004;5(2):R12.
47. Feldgarden M, Brover V, Gonzalez-Escalona N, Frye JG, Haendiges J, Haft DH, et al. AMRFinderPlus and the Reference Gene Catalog facilitate examination of the genomic links among antimicrobial resistance, stress response, and virulence. Sci Rep. 2021;11(1):12728.
48. Bonin N, Doster E, Worley H, Pinnell LJ, Bravo JE, Ferm P, et al. MEGARes and AMR++, v3.0: an updated comprehensive database of antimicrobial resistance determinants and an improved software pipeline for classification using high-throughput sequencing. Nucleic Acids Res. 2023;51(D1):D744–52.
49. Camargo AP, Roux S, Schulz F, Babinski M, Xu Y, Hu B, et al. Identification of mobile genetic elements with geNomad. Nat Biotechnol. 2024;42(8):1303–12.
50. NIH Comparative Genomics Resource (CGR) - NCBI - NLM.
51. Page AJ, Cummins CA, Hunt M, Wong VK, Reuter S, Holden MTG, et al. Roary: rapid large-scale prokaryote pan genome analysis. Bioinformatics. 2015;31(22):3691–3.
52. Nguyen LT, Schmidt HA, von Haeseler A, Minh BQ. IQ-TREE: a fast and effective stochastic algorithm for estimating maximum-likelihood phylogenies. Mol Biol Evol. 2015;32(1):268–74.
53. Kalyaanamoorthy S, Minh BQ, Wong TKF, von Haeseler A, Jermiin LS. ModelFinder: fast model selection for accurate phylogenetic estimates. Nat Methods. 2017;14(6):587–9.
54. Sayers E. A General Introduction to the E-utilities. In: Entrez Programming Utilities Help. National Center for Biotechnology Information (US); 2022.
55. Letunic I, Bork P. Interactive Tree of Life (iTOL) v6: recent updates to the phylogenetic tree display and annotation tool. Nucleic Acids Res. 2024;gkae268.
56. Xu M, Li Y, Shi Y, Liu H, Tong X, Ma L, et al. Molecular epidemiology of Mycoplasma pneumoniae pneumonia in children, Wuhan, 2020–2022. BMC Microbiol. 2024;24:23.
57. Seemann T. Prokka: rapid prokaryotic genome annotation. Bioinformatics. 2014;30(14):2068–9.
58. Hsieh YC, Li SW, Chen YY, Kuo CC, Chen YC, Chang IYF, et al. Global Genome Diversity and Recombination in Mycoplasma pneumoniae. Emerg Infect Dis. 2022;28(1):111–7.
59. Voronina EN, Gordukova MA, Turina IE, Mishukova OV, Dymova MA, Galeeva EV, et al. Molecular characterization of Mycoplasma pneumoniae infections in Moscow from 2015 to 2018. Eur J Clin Microbiol Infect Dis. 2020;39(2):257–63.
60. Jacobs E, Ehrhardt I, Dumke R. New insights in the outbreak pattern of Mycoplasma pneumoniae. Int J Med Microbiol. 2015;305(7):705–8.
61. Uldum SA, Bangsborg JM, Gahrn-Hansen B, Ljung R, Mølvadgaard M, Føns Petersen R, et al. Epidemic of Mycoplasma pneumoniae infection in Denmark, 2010 and 2011. Euro Surveill. 2012;17(5):20073.
62. Beeton ML, Zhang XS, Uldum SA, Bébéar C, Dumke R, Gullsby K, et al. Mycoplasma pneumoniae infections, 11 countries in Europe and Israel, 2011 to 2016. Euro Surveill. 2020;25(2):1900112.
63. Meyer Sauteur PM, Krautter S, Ambroggio L, Seiler M, Paioni P, Relly C, et al. Improved Diagnostics Help to Identify Clinical Features and Biomarkers That Predict Mycoplasma pneumoniae Community-acquired Pneumonia in Children. Clin Infect Dis. 2020;71(7):1645–54.
64. Choo S, Lee YY, Lee E. Clinical significance of respiratory virus coinfection in children with Mycoplasma pneumoniae pneumonia. BMC Pulm Med. 2022;22:212.
65. Michelow IC, Olsen K, Lozano J, Rollins NK, Duffy LB, Ziegler T, et al. Epidemiology and clinical characteristics of community-acquired pneumonia in hospitalized children. Pediatrics. 2004;113(4):701–7.
66. Toikka P, Juvén T, Virkki R, Leinonen M, Mertsola J, Ruuskanen O. Streptococcus pneumoniae and Mycoplasma pneumoniae coinfection in community acquired pneumonia. Arch Dis Child. 2000;83(5):413–4.
67. Heiskanen-Kosma T, Korppi M, Jokinen C, Kurki S, Heiskanen L, Juvonen H, et al. Etiology of childhood pneumonia: serologic results of a prospective, population-based study. Pediatr Infect Dis J. 1998;17(11):986–91.
68. Korppi M. Mixed microbial aetiology of community-acquired pneumonia in children. APMIS. 2002;110(7–8):515–22.
69. Guo Q, Li L, Wang C, Huang Y, Ma F, Cong S, et al. Comprehensive virome analysis of the viral spectrum in paediatric patients diagnosed with Mycoplasma pneumoniae pneumonia. Virol J. 2022;19(1):181.
70. Søndergaard MJ, Friis MB, Hansen DS, Jørgensen IM. Clinical manifestations in infants and children with Mycoplasma pneumoniae infection. PLoS ONE. 2018;13(4): e0195288.
71. Zhao J, Xu M, Tian Z, Wang Y. Clinical characteristics of pathogens in children with community-acquired pneumonia were analyzed via targeted next-generation sequencing detection. PeerJ. 2025;13: e18810.
72. Li N, Qiang G feng, Liu R han, Meng L lan, Ning J, Shen C qing, et al. Analysis of clinical characteristics of severe mycoplasma pneumoniae pneumonia complicated with virus infection in children. Research Square; 2024.
73. Chi J, Tang H, Wang F, Wang Y, Chen Z. Surge in Mycoplasma Pneumoniae infection and Respiratory Viruses Co-infection in Children With Community-Acquired Pneumonia in the Post-Pandemic. Pediatric Health Med Ther. 2024;15:279–88.
74. Wang N, Xu X, Xiao L, Liu Y. Novel mechanisms of macrolide resistance revealed by in vitro selection and genome analysis in Mycoplasma pneumoniae. Front Cell Infect Microbiol. 2023May;22(13):1186017.
75. Kim K, Jung S, Kim M, Park S, Yang HJ, Lee E. Global Trends in the Proportion of Macrolide-Resistant Mycoplasma pneumoniae Infections: A Systematic Review and Meta-analysis. JAMA Netw Open. 2022;5(7): e2220949.
76. Loconsole D, De Robertis AL, Sallustio A, Centrone F, Morcavallo C, Campanella S, et al. Update on the Epidemiology of Macrolide-Resistant Mycoplasma pneumoniae in Europe: A Systematic Review. Infect Dis Rep. 2021;13(3):811–20.
77. Ferguson GD, Gadsby NJ, Henderson SS, Hardie A, Kalima P, Morris AC, et al. Clinical outcomes and macrolide resistance in Mycoplasma pneumoniae infection in Scotland. UK J Med Microbiol. 2013;62(Pt 12):1876–82.
78. Waites KB, Ratliff A, Crabb DM, Xiao L, Qin X, Selvarangan R, et al. Macrolide-Resistant Mycoplasma pneumoniae in the United States as Determined from a National Surveillance Program. J Clin Microbiol. 2019;57(11):e00968-e1019.
79. Guo D, Hu W, Xu B, Li J, Li D, Li S, et al. Allele-specific real-time PCR testing for minor macrolide-resistant Mycoplasma Pneumoniae. BMC Infect Dis. 2019;19:616.
80. Qu J, Chen S, Bao F, Gu L, Cao B. Molecular characterization and analysis of Mycoplasma pneumoniae among patients of all ages with community-acquired pneumonia during an epidemic in China. Int J Infect Dis. 2019;83:26–31.
81. Wang N, Zhang H, Yin Y, Xu X, Xiao L, Liu Y. Antimicrobial Susceptibility Profiles and Genetic Characteristics of Mycoplasma pneumoniae in Shanghai, China, from 2017 to 2019. Infect Drug Resist. 2022;15:4443–52.
82. Wang G, Wu P, Tang R, Zhang W. Global prevalence of resistance to macrolides in Mycoplasma pneumoniae: a systematic review and meta-analysis. J Antimicrob Chemother. 2022;77(9):2353–63.
83. Lee JK, Choi YY, Sohn YJ, Kim KM, Kim YK, Han MS, et al. Persistent high macrolide resistance rate and increase of macrolide-resistant ST14 strains among Mycoplasma pneumoniae in South Korea, 2019–2020. J Microbiol Immunol Infect. 2022;55(5):910–6.

84. Tanaka T, Oishi T, Miyata I, Wakabayashi S, Kono M, Ono S, et al. Macrolide-Resistant Mycoplasma pneumoniae Infection, Japan, 2008–2015. Emerg Infect Dis. 2017;23(10):1703–6.
85. Spuesens EBM, Fraaij PLA, Visser EG, Hoogenboezem T, Hop WCJ, van Adrichem LNA, et al. Carriage of Mycoplasma pneumoniae in the upper respiratory tract of symptomatic and asymptomatic children: an observational study. PLoS Med. 2013;10(5): e1001444.
86. Meyer Sauteur PM, Unger WWJ, Nadal D, Berger C, Vink C, van Rossum AMC. Infection with and Carriage of Mycoplasma pneumoniae in Children. Front Microbiol. 2016;7:329.
87. Daxboeck F, Krause R, Wenisch C. Laboratory diagnosis of Mycoplasma pneumoniae infection. Clin Microbiol Infect. 2003;9(4):263–73.

Publisher's Note